Elleouet et al. *New Zealand Journal of Forestry Science* (2025) 55:15
https://doi.org/10.33494/nzjfs552025x434x
E-ISSN: 1179-5395
published on-line: 25/09/2025

RESEARCH ARTICLE Open Access

New Zealand Journal of Forestry Science

Quantifying radial growth loss from red needle cast in *Pinus radiata* D.Don plantations

Joane S. Elleouet[1,*,†], David W. Lane[2,†], Lindsay S. Bulman[3], Yvette L. Dickinson[4] and Stuart Fraser[4]

[1] *Bioeconomy Science Institute, Scion Group, Level 6, 17-21 Whitmore Street, Wellington Central 6011, New Zealand*
[2] *Bioeconomy Science Institute, Scion Group, Private Bag 3020, Rotorua 3046, New Zealand (Currently: Department of Primary Industries, 21-23 Redden Street, Cairns QLD 4870, Australia)*
[3] *Bioeconomy Science Institute, Scion Group, Private Bag 3020, Rotorua 3046, New Zealand (Currently: 46 Matipo Avenue, Rotorua 3015, New Zealand)*
[4] *Bioeconomy Science Institute, Scion Group, Titokorangi Drive, Private Bag 3020, Rotorua 3046, New Zealand*

† Equal contributions of authors

*Corresponding author: Joane.Elleouet@scionresearch.com

(Received for publication 15 December 2024; accepted in revised form 19 August 2025)
Editor: Horacio E. Bown

Abstract

Background: Red needle cast (RNC), caused by *Phytophthora pluvialis* Reeser, W.L. Sutton & E.M. Hansen, is a significant foliar disease impacting *Pinus radiata* D.Don in New Zealand. First detected in 2005, the disease has now been observed in all regions of the country. In the most severe cases, defoliation of entire tree crowns can occur at a landscape scale. While some evidence of growth loss and productivity reduction has been reported, quantitative estimates of the effect of RNC on productivity are needed to inform disease management and mitigation decisions. This study aims to assess both short- and long-term losses in radial growth due to RNC.

Methods: We used tree cores to quantify yearly basal area increments at two plantations: a 32-year-old stand in Wharerata Forest, with documented history of outbreaks both severe and cyclic in nature, and a 26-year-old stand in Kinleith Forest, where 8 years of continuous disease severity monitoring has been conducted at the tree level. A Bayesian multilevel modelling framework was used to predict growth losses due to RNC at each site separately, accounting for yearly weather and outbreak severity.

Results: We predicted a 31% to 51.5% radial growth loss in the year following an RNC outbreak, with reduced growth detectable for 3 to 4 years after disease, amounting to up to 30.6% growth loss over the course of a single event. Recurring disease events every three to four years can lead to a 20% reduction in total radial area growth over the period encompassing the presence of the disease, with no evidence that each additional RNC event aggravates growth loss.

Conclusions: RNC causes significant growth loss in *P. radiata*, with the potential to severely reduce stand productivity over a rotation period. These results contribute valuable insights for forest managers in RNC-prone regions. The enablement of more accurate productivity forecasts and targeted mitigation efforts will also benefit from further research on the impact of RNC on other important tree characteristics such as wood density, and the interaction of disease presence and impact with climate.

Keywords: Radiata pine; disease; red needle cast; *Phytophthora pluvialis*; basal area increment; growth loss; multilevel Bayesian model

Introduction

Red needle cast (RNC), a foliar disease of radiata pine (*Pinus radiata* D.Don) caused by *Phytophthora pluvialis* Reeser, W.L. Sutton & E.M. Hansen, and occasionally *Phytophthora kernoivae* Brasier, Beales & S.A. Kirk, can cause dramatic needle loss in New Zealand commercial forests. The disease was first observed in radiata pine forests in the Gisborne region on the east coast of New Zealand's North Island in 2005 (Dick et al. 2014) and has now been reported in all regions of the country. RNC may impact tree growth and wood characteristics, however, its impact has not been fully assessed. Here, we aim to quantify the growth loss and recovery time associated with RNC in New Zealand radiata pine forests.

At the needle level, symptoms of RNC start as olive green-coloured lesions that turn khaki-coloured, spread along the needle while turning red/brown, before eventual needle senescence and premature loss. New needle growth in the following growing season is generally believed to not be affected. At the tree level, the disease affects mature needles of the lower crown and spreads towards the upper canopy. Symptoms appear in late autumn or winter depending on year and location (Dick et al. 2014). Outbreaks vary in severity across regions and years. Severe outbreaks can affect plantations at the regional scale and lead to defoliation of whole tree crowns, as observed on several occasions in the Gisborne region of the North Island (Watt et al. 2024; Fraser et al. 2025). In contrast to other foliar diseases primarily affecting younger trees in New Zealand such as Dothistroma needle blight caused by *Dothistroma septosporum* (Dorog.) M. Morelet, RNC affects trees at all ages from 4 years old to rotation age, with higher severity in trees over 10 years old (Dick et al. 2014). Anecdotally, an outbreak frequency of roughly three years has been observed over the past two decades in the most affected forests in the Gisborne region. Bearing in mind that the disease primarily impacts older foliage and that radiata pine needles generally have a 3-year lifecycle, this outbreak frequency could be at least partially explained by the time needed for a full tree crown to develop from new foliar growth. Concomitant with the seemingly cyclical behaviour of the disease in affected areas, extent and severity of RNC outbreaks can partially be predicted based on current year's weather conditions, with outbreaks more likely to occur after wet and relatively cool summers (Watt et al. 2024).

There is widespread evidence of other conifer foliar diseases impacting tree growth in New Zealand commercial plantations. In juvenile radiata pine, Dothistroma needle blight causes minimal growth loss until approximately 25% of the foliage is infected. Beyond this threshold, growth loss increases proportionally with infection level up to 75%, at which point growth nearly halts. Radiata pine over 15 years old are rarely affected (Bulman et al. 2013). Cyclaneusma needle cast, caused by *Cyclaneusma minus* (Butin) DiCosmo, Peredo & Minter, affects radiata pine trees up to age 20 and can cause a volume increment loss of 60% at an 80% average severity score (Bulman 1993). Swiss needle cast, caused by *Nothophaeocryptopus gaeumannii* (T. Rohde) Videira, C. Nakash., U. Braun & Crous 2017, affects Douglas-fir plantations internationally, and its effect on growth in New Zealand has been quantified to a cumulative mean reduction of 25% for mean top height, 27% for basal area, and 32% for stem volume, with variations around these estimates in different regions (Kimberley et al. 2011).

As RNC leads to premature defoliation and can affect whole stands repeatedly throughout a rotation, it is highly likely that large-scale outbreaks have a negative effect on tree growth and, ultimately, stand productivity. The fact that it affects mature, final-crop trees makes it likely to cause larger absolute volume growth losses than other diseases that affect younger trees. It is therefore necessary to assess the effects of RNC on growth and other tree characteristics to predict losses and enable cost-benefit analyses of potential treatments and breeding efforts. The first quantification of the effect of RNC on tree growth suggested that a high-severity disease event can lead to a 38% growth loss the following year, and a 16% growth loss over 3 years (Beets, unpublished data).

As the disease has now been expressing in New Zealand for at least two decades, observations of RNC have accumulated and data is available to precisely quantify the effect of disease severity and frequency on radiata pine growth. Here, we focus on two case studies in the North Island of New Zealand to assess each of these aspects of the disease at different timescales and resolution, using tree cores to quantify yearly radial growth. In the first case study, we assess the short- and long-term effects of frequently occurring outbreaks over the rotation of a 32-year-old stand in Wharerata Forest in the Gisborne region. The second case study addresses a finer spatial and temporal scale to quantify the effect of tree-level severity of one RNC outbreak over 4 years in a mature stand located in Kinleith Forest (central North Island). The two sites associated with these case studies are subsequently referred to as "Wharerata" and "Kinleith".

Methods

Study sites and sampling design

Wharerata

A radiata pine stand located at Maxwells Road (-38.90, 177.83) in Wharerata was used to infer the effect of repeated RNC events on growth over the course of a rotation at the stand level.

Wharerata is a coastal, high elevation (up to c. 600 m), steep land commercial forest south of Gisborne on the East coast of the North Island. The Maxwells Road site is situated on a flat area, at c. 530 m elevation, 6 km from the coast. The soils are a mix of well drained loam over sand, classified as Humose Orthic Podzols according to the New Zealand Soil Classification system (Hewitt 2010) and imperfectly drained silt, classified as Mottled Orthic Brown Soils (Landcare Research NZ 2019). Mean annual temperature is 11.7 degrees Celsius, mean total annual

rainfall is 1599 mm. The trees were planted in 1990, and pruning and thinning activities were conducted in the stand prior to 2002. Stand density was 317 stems per hectare after the last thinning event.

Although RNC symptoms have only been visually confirmed in this specific stand in 2011 (Beets, unpublished data), there is compelling evidence that RNC outbreaks affected the stand in 2005, 2008, 2011, 2014, 2017, and 2021. RNC outbreaks were observed in the region for the first time in 2005 and again in 2008 (Dick et al. 2014). The dramatic growth reductions observed in the tree ring series the year after these two years could be due to drought, but local yearly and seasonal climate records do not show lower than average rainfall for these years. Besides, data from additional tree coring at stands in the vicinity (not included in this analysis) do not show those dips, which suggest the cause of growth reduction acts at a finer spatial scale than climatic factors, typical of disease outbreaks. Dothistroma needle blight is the other common disease in the area and can also cause growth reductions, but by 2005 the stand was over 15 years old, and therefore not prone to this disease which mostly affects stands under this age. In 2014, forest health monitoring activities performed in another forest stand at Maxwells Road positively identified an abundance of *Phytophthora pluvialis* on needle samples (Fraser et al. 2020). Finally, between 2015 and 2024 a stand opposite to one studied on Maxwells Road was monitored yearly for disease, and 85% and 90% of monitored trees had RNC symptoms in 2017 and 2021 respectively. The stand analysed here has been noted as the most frequently and severely affected by disease by local forest managers. As a result, RNC observations performed at the same site (2014, 2017, 2021) or in the region (2005, 2008) together with dips in tree ring series the following year are a compelling argument to assume that an outbreak occurred at the stand in those years. We therefore identified a total of 6 outbreaks following a 3-year cycle, apart from the 2021 event which occurred 4 years after the 2017 event.

Tree cores were collected from September to December 2022, 32 years after the stand was established. Four sampling plots were defined in the Maxwells Road stand in Wharerata, between 35 and 70 metres from the road, along a stretch of 350 metres. In each plot, at least 10 trees were selected for coring within a 10-meter radius from the plot centre. Trees with trunk abnormalities were avoided. Selected trees were cored at about 50cm from the ground to avoid compromising wood quality and multiple cores on different sides of each tree were collected. The total number of trees from Wharerata used in the final analysis was 39.

Kinleith

To assess the effect of RNC severity on growth over one disease event at the tree level, a radiata pine stand in Kinleith (-38.22, 175.93) that was affected by RNC in 2016 was selected. RNC outbreak history prior to 2016 is not known at this site.

Kinleith is an inland, large contiguous radiata pine plantation, ranging 350-800 m elevation in the Central North Island of New Zealand. The site is situated in a flat area, at c. 420 m elevation. The soil is well drained silt, classified as Typic Orthic Allophanic Soils according to the New Zealand Soil Classification system (Hewitt 2010; Landcare Research NZ 2019). Mean annual temperature is 12.1 degrees Celsius, mean total annual rainfall is 1667 mm. The trees were planted in 1995 (plot 4), and 1996 (plots 1-3), with thinning occurring at year 6 (2001 in plot 4 and 2002 in plots 1-3). Stand density was 355 stems per hectare after thinning.

RNC severity scores for individual trees were obtained in November 2016 as the percentage of the unsuppressed crown with red colouration, in 5% intervals from 0 to 100%. The stand was monitored and scored for disease in spring (September-October) each subsequent year until 2021. Four 20-tree plots with 2016 RNC scores available were selected for coring. Wood cores were sampled in November 2020 for plot 1 and 2, and May 2021 for plot 3 and 4. This corresponds to 25-26 years after establishment. Selected trees were cored at breast height, and multiple cores on different sides of each tree were collected. The total number of trees from Kinleith used in the final analysis was 77.

Wood core processing and data extraction

Cores were sanded down using fine grit sandpaper and oiled with orange oil or standard kitchen-bench wood oil so that the growth bands of the late-wood were distinct. The cores were then scanned in a high-resolution scanner and measured using the software GIMP (https://www.gimp.org/). Not all cores included the pith, mainly due to the large diameter of selected trees. In cases where the cores were offset from the pith, the following correction method was applied estimating the radius of the last visible ring (Figure 1). A circle was fitted through the two points of the last ring intersected by the wood core and the deviation from the pith was measured from this circle. Basic trigonometry allowed the calculation of each corrected cumulative ring width from the pith. As the first visible ring from the pith may not be the actual first ring, the corrected measurement for the first visible ring of each core was not used in subsequent processing. Corrected ring widths were averaged over all available cores of each tree to obtain one ring-width series per tree. Basal area and basal area increment series were subsequently calculated from ring-width series. Analyses were restricted to the post-2005 period (starting at stand age 15 at Wharerata and age 9-10 at Kinleith), to avoid the confounding effects of silvicultural activities.

Basal area growth modelling

The modelling objective was to assess the effect of stand-level RNC presence/absence each year (Wharerata) and the effect of tree-level RNC severity (Kinleith) on radial growth in subsequent years. The Bayesian models developed here are ultimately used to predict and quantify yearly growth loss following disease, overall growth loss from each RNC event, and growth loss across a whole rotation in a stand experiencing a high-frequency RNC cycle. The output of a Bayesian statistical model is

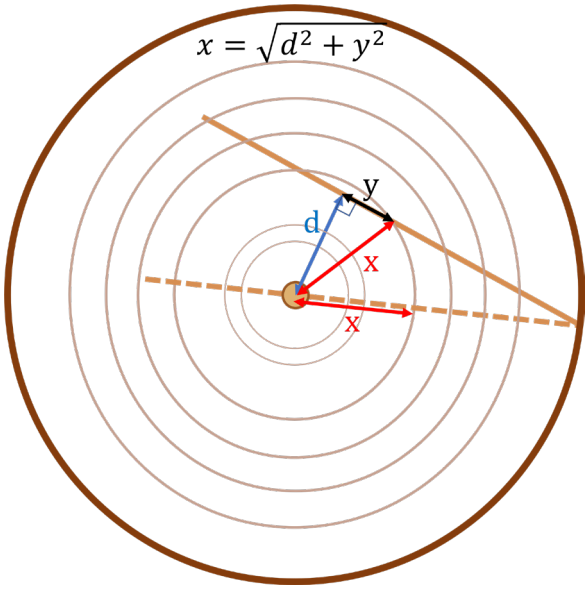

FIGURE 1: Cumulative ring width correction method for cores deviating from the pith. This schematic corresponds to a tree stem section at coring height, showing tree rings and bark. The original ring width measurement "y" on the wood core (full light-brown segment) is corrected to an estimated distance to the pith "x" using the formula stated at the top, where "d" is obtained by a fitting a circle through the two points of the last ring intersected by the wood core. The dashed light-brown line represents the corrected wood-core position. The same process is applied to cumulative ring widths for all years from the pith to the bark.

a probability distribution that quantifies the uncertainty about the estimated quantities of interest, called the posterior distribution. The Bayesian framework was an advantageous choice in this exercise as it naturally accommodates the multilevel nature of the data where tree ring series represent longitudinal measurements on individual trees. Also, relevant results from our models required mathematically transforming estimated quantities, for which uncertainties can be defined by conducting the transformations on the whole posterior distribution and subsequently summarising the obtained posterior distribution for the quantity of interest into credible intervals. Obtaining estimates of interest and their uncertainty bounds relied on integration over individual (fixed) and group (random) effects. This is naturally handled in a Bayesian framework that uses a Markov Chain Monte Carlo (MCMC) algorithm, where a sample for the posterior distribution is obtained, through averaging over variable values for each iteration of the posterior sample (fixed effects) or through Monte-Carlo integration (random effects).

All analyses and visualisation were performed using R (R Core Team, 2023) and statistical models were fitted using the brms package version 2.20.1 (Bürkner, 2017). This package uses Stan's Hamiltonian Monte Carlo (HMC) algorithm which is an efficient type of MCMC (Stan Development Team 2023). Model convergence was assessed using visual inspection of traceplots of Hamiltonian Monte Carlo (HMC) chains and assessment of the Gelman-Rubin convergence criterion. Chain resolution was assessed using bulk and tail estimated sample sizes (ESS). HMC computation details and performance for each site's final model are described in Table 1. Predictor selection was performed using the LOOIC criterion from Leave-one-out Cross-Validation approximated by Pareto-smoothed importance sampling (Vehtari, 2017). As the Bayesian paradigm does not support the implementation of statistical tests, we do not report any p-values or significance. Bayesian models directly estimate quantities of interest through a probability distribution. We summarised these distributions by their mean as well as 90% credible intervals which are defined as the interval between the 5% and 95% percentiles of the posterior distribution. An alternative to the frequentist concept of significance would be to assess whether 90% credible interval overlap 0 (or the equivalent of a null hypothesis value). If there is no overlap, then one can say that there is less that 90% probability that the quantity of interest is the null value.

Wharerata growth model

As we were unable to identify radiata pine stands unaffected by RNC at the Wharerata site, we lacked growth data from healthy stands corresponding to the study period and location to use as a reference. Therefore, we used a radial tree growth series derived from the 300 Index, called the 300 Index growth model, as an RNC-free reference for Wharerata plots. The 300 Index is a measure of stand productivity, defined as the stem volume mean annual increment at age 30 for a stand density of 300 stems ha^{-1} and standard silvicultural treatments (Kimberley et al. 2005). The 300 Index growth model has been a part of the estimation process of the 300 Index (Kimberley et al. 2005). It is a

TABLE 1: Hamiltonian Monte Carlo (HMC) parameters and chain diagnostics used in the final Kinleith and Wharerata models. $\hat{R}$: Gelman-Rubin convergence criterion; ESS: estimated sample size.

Model	Number of HMC chains	HMC chain length	HMC warmup length	Size of final posterior sample	Maximum tree depth	Target acceptance probability	Maximum $\hat{R}$	Minimum bulk ESS	Minimum tail ESS
Wharerata	4	9000	6000	1000	12	0.99	1.01	414	915
Kinleith	4	5000	4000	1000	10	0.8	1	2254	1421

nonlinear function of age, stocking density, silvicultural activities and site productivity. Once the 300 Index has been established for a site, the model can therefore be used to predict basal area for any stand age and stocking density. We extracted estimates of the 300 Index at each plot location using a New Zealand–wide index map which relies on a database of 3,676 plots and kriging techniques involving terrain attributes (Watt et al. 2021). We then input each plot's 300 index, initial stocking density and silvicultural activities into the 300 Index growth model described in Kimberley et al. (2005) to create a plot-level 32-year reference growth series. As the model outputs basal area predictions for each year of growth at the stand level and takes into account tree mortality by decreasing the stand density in time, we derived an average individual tree basal area for each year of growth by dividing stand basal area by the estimated stand density, obtaining for any given year i and an average tree a value z_i of basal area increment at the Wharerata site.

Basal area increment y_{ij} for each year i and each measured tree j at Wharerata was divided by the reference z_i from the corresponding tree age. We define the random variable R where: $R_{ij} = y_{ij} / z_i$ for a given tree j and year i and modelled the logarithm of this ratio using a Bayesian hierarchical linear model, with the variables described in Table 2 as predictors. The model with lowest LOOIC is described in the equations below and included as predictors the two first climate principal components (PC_1 and PC_2), RNC event number (E), and two binary variables, RNC_1 and RNC_2, stating whether there had been an RNC outbreak at each of the two previous years. As outbreaks occurred every three years for most of the study period, we lacked data to directly assess the effect of RNC at each year beyond 3 years of growth post-disease. Tree was added as a group-level covariate to account for the longitudinal nature of the data. Plot as a group-level variable was left out as it did not improve model LOOIC. The model is as follows:

$$\log(R_{ij}) \sim N(\mu_{ij}, \sigma^2)$$

$$\mu_{ij} = \alpha + \alpha_{Tj} + \beta_{PC1}PC_{1i} + \beta_{PC2}PC_{2i} + \beta_E E_i + \beta_{RNC1}RNC_{1i} + \beta_{RNC2}RNC_{2i}$$

where α is the grand mean, α_T the tree-level random effect with distribution $\alpha_{Tj} \sim Normal(\mu_T, \sigma_T^2)$, and all other terms corresponding to variables described in Table 2 and their associated β coefficients. Standard normal priors (truncated to positive values for standard deviation parameters σ and σ_T) were used for all parameters in the model. We define p_0 as the obtained posterior distribution of expected values for observations, where:

$$p_{0 =} p(\log(R)|\alpha, \alpha_T, \beta_{PC1}, \beta_{PC2}, \boldsymbol{\beta_E}, \beta_{RNC1}, \beta_{RNC2})$$

The quantity of interest for prediction is the growth loss experienced by an average tree in the 3 years following each RNC outbreak, assuming average climate

TABLE 2: Explanatory variables used in the models. "Level" refers to the individual entities described by the variable, and "model" states whether the variable is used in the Wharerata model (W) or the Kinleith model (K), or both. The variable appears bold if it is included in the final Wharerata model and underlined if it is included in the final Kinleith model.

Variable	Variable Name	Type	Level	Description	Model
PC1, **PC2**, PC3	Climate principal components	continuous	year	Principal components from a PCA performed on ClimateAP monthly, seasonal, and annual variables (Wang et al. 2017) for the plot's geographic location.	W, K
YSTD	Standardised year of growth	continuous	year	Year, ranging from 2005 to 2022 at Wharerata and 2005 to 2022 at Kinleith, scaled and centred.	W, K
E	RNC event number	categorical	year	For a given year, takes the value corresponding to the most recent event. Six disease events occurred throughout the rotation.	W
RNC1, RNC2	RNC year	binary	year	States whether there had been an RNC outbreak 1 or 2 years prior. For instance, for a given year, RNC1 takes the value 1 if RNC was present the year prior, 0 otherwise.	W
S1, S2, S3, S4	RNC severity scores for years 1,2,3 and 4 prior	continuous	tree*year	Scores ranging from 0 to 100. This set of variables reflects both the number of years since the outbreak (variable index) and each tree's severity (variable value). For instance, for a given tree and year, S2 would record the RNC severity level experienced by that tree 2 years prior to that year.	K

conditions. We define the posterior for this quantity p_{pred}, where:

$$p_{pred} = p((R)|\alpha, \boldsymbol{\beta_E}, \beta_{RNC1}, \beta_{RNC2})$$

To obtain p_{pred} from p_0, we first calculate the growth loss experienced by an average tree in the 3 years following each RNC outbreak conditioning on observed climate conditions, by integrating over the random variable representing tree effects:

$$p_1 = p(R|\alpha, \beta_{PC1}, \beta_{PC2}, \boldsymbol{\beta_E}, \beta_{RNC1}, \beta_{RNC2})$$

$$= \int e^{p_0}\, d\alpha_T$$

To perform this integration on the MCMC sample of p_0, we use a Monte-Carlo integration where the following process was iterated for each of the 1000 posterior iterations:

1. For each observation, calculate the "fixed" part of the predictor using parameter estimates from the corresponding posterior iteration
2. simulate a sample of 100 tree effects from $\alpha_{Tj} \sim Normal(\mu_T, \sigma_T^2)$
3. calculate the expected predictor value for these 100 simulations
4. exponentiate the obtained value
5. average over the 100 values to obtain a unique value for the current posterior iteration.

Finally, to obtain p_{pred}, we marginalised the posterior p_1 over climate effects by averaging all predictions with identical (E, $RNC1$, $RNC2$) values but different ($PC1$, $PC2$) values.

$$p_{pred} = \int p_1\, d(\beta_{PC1}, \beta_{PC2})$$

The obtained posterior distribution p_{pred} was summarised using means and 5% and 95% quantiles to obtain 90% credible intervals.

Kinleith growth model

We define the random variable Y corresponding to the percentage of total area growth for each tree. We have $Y_{ij} = y_{ij} / y_j^{tot}$ where y_{ij} is the stem area increment for a given year i and measured tree j and y_j^{tot} is the total basal area increment for tree j. The logarithm of this Y was modelled using a Bayesian hierarchical linear model, with the variables described in Table 2 as predictors. The model with lowest LOOIC is described in the equations below and included as predictors year of growth (YSTD), the three first climate principal components (PC_1, PC_2 and PC_3), and RNC severity scores for years 1,2,3 and 4 prior to year i (S1-S4). Tree was added as a group-level covariate but plot was left out as it did not improve model LOOIC. The model is as follows:

$$\log(Y_{ij}) \sim N(\mu_{ij}, \sigma^2)$$

$$\mu_{ij} = \alpha + \alpha_{Tj} + \beta_{YSTD} YSTD_i + \beta_{PC1} PC_{1i} + \beta_{PC2} PC_{2i} + \beta_{PC3} PC_{3i} + \beta_{S1} S_{1i} + \beta_{S2} S_{2i} + \beta_{S3} S_{3i} + \beta_{S4} S_{4i}$$

where α is the grand mean, α_T is the tree-level random effect with distribution $\alpha_j \sim Normal(\mu_T, \sigma_T^2)$, and all other terms fixed terms described in Table 2. Normal priors with mean 0 and standard deviation 0.5 (truncated to positive values for standard deviation parameters σ and σ_T) were used for all parameters in the model, apart from which had a normal prior with mean 1 and standard deviation 0.5. We define as the obtained posterior distribution of observations, where:

$$p_0 = p(\log(Y)|\alpha, \alpha_T, \beta_{YSTD}, \beta_{PC1}, \beta_{PC2}, \beta_{PC3}, \beta_{s1}, \beta_{s2}, \beta_{s3}, \beta_{s4})$$

To quantify growth loss due to RNC, we first calculate the posterior for the expected relative growth experienced by an average tree in the 4 years following the 2016 RNC outbreak at three different 2016 severity scores (0%, 50%, and 95%,). We define this posterior as , where:

$$p_{1\,=} p(Y|\alpha, \alpha_T, \beta_{YSTD}, \beta_{PC1}, \beta_{PC2}, \beta_{PC3}, \beta_{s1}, \beta_{s2}, \beta_{s3}, \beta_{s4})$$

$$= \int e^{p_0}\, d\alpha_T$$

To calculate p_1, we first calculate predictions from the fitted model for a simulated dataset of trees, for growth years 2016 to 2020 and combinations of S1-S4 variables mimicking no symptoms (0%), moderate severity (50%), and high severity (95%) in 2016, and no symptoms the following years. Similarly to the Wharerata model, we perform the integration over tree effects using the Monte-Carlo procedure described below, for each of the 1000 posterior iterations of predictions.

1. For each prediction calculate the "fixed" part of the predictor using parameter estimates from the corresponding posterior iteration
2. simulate a sample of 100 tree effects from $Normal(\mu_T, \sigma_T^2)$
3. calculate the predictor value for these 100 simulations
4. exponentiate the obtained value
5. average over the 100 values to obtain a unique value for the current posterior iteration.

We obtained a posterior prediction for relative growth for each combination of year (2016-2020) and 2016 RNC severity (0%, 50%, 95%). Finally, to be able to isolate the effect of RNC and year post-disease from the effect of climate variables, for each growth year 2016-2020, we standardised the posterior distribution for the medium and high severity by dividing each of their posterior iteration by the corresponding iteration from the prediction of 0% severity.

The obtained distribution of affected-to-healthy predicted growth proportion per year and RNC severity (50% and 95%) was summarised by extracting the mean, 5%, and 95% percentiles to obtain 90% credible intervals.

Results

Observed growth compared to the 300 Index reference at Wharerata

We observed a wide variation in overall growth among sampled trees at Wharerata (Figure 2a). Out of 39 trees, 35 exhibited lower overall growth than the 300 Index growth reference over the rotation (Figure 2a). However, the observed yearly growth increment (Figure 2b) was not consistently lower than the reference, with an apparent cyclic pattern showing an alternance of low growth years where most if not all trees grew less than the reference (e.g. 2009), and high growth years, where trees on average grew as much or more than the reference (e.g. 2017, 2021).

Inferred growth response to RNC at Wharerata forest

The final model related relative growth (on a logarithmic scale) to year, climate, and disease incidence. All HMC chains converged, with an appropriate posterior resolution (Table 1). The model revealed a major effect of disease on subsequent yearly growth over the 3 years following an outbreak. Figure 3 shows the summarised posterior distributions of the yearly radial growth relative to expectation from a reference, for each year up to three years after the 6 disease events, and after controlling for tree and climate effects. Predictions confirm that trees were growing as expected from the reference in 2005, the year of the first RNC event. The cyclic pattern of inferred RNC-related growth patterns matched the pattern observed in the raw data on Figure 2b, suggesting that RNC incidence was the most important driver of growth differences among years.

The necessary inclusion of RNC event number in the final model suggests that growth loss varied from one event to another, likely due to different levels of outbreak intensity. The inclusion of RNC event number as a factor in the model also allowed differentiation of growth patterns between years other than 1 or 2 years before an outbreak. For instance, 2005 (no prior outbreak) and other outbreak years (mainly 3 years after an outbreak) could be differentiated and therefore an indication of growth loss past 2 years after an outbreak could be gained without specifically creating predictors for those years.

Percent estimated growth loss due to RNC for each year following disease is shown in Table 3. At each RNC event, the trees on average grew up to 51.5% less than the reference the year after disease, up to 35.2% less than the reference two years after disease, and up to 9% less than the reference three years after disease. Only for year 2021 were growth patterns 4 years after disease able to be observed (outbreak 5) and the model did not detect any growth difference from the reference on average for that year, providing some evidence that trees might need a total of three to four years to recover from an RNC outbreak. The model also provides no evidence

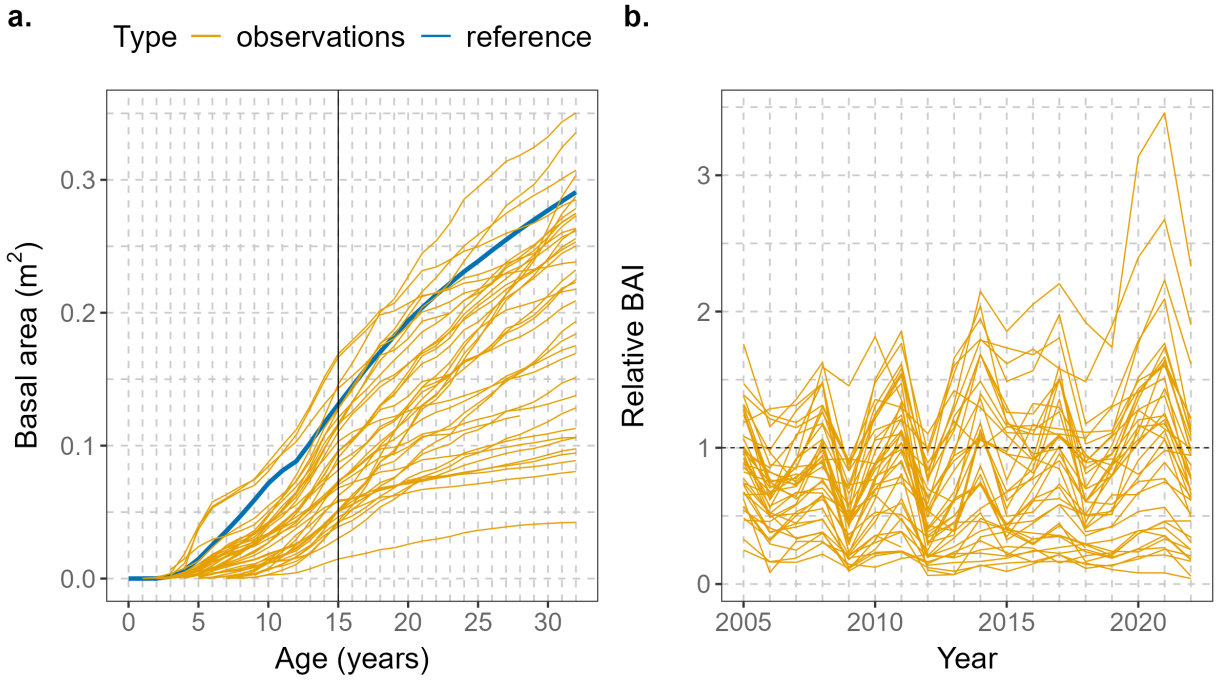

FIGURE 2: a. Cumulative basal area growth over the rotation for 39 trees at Maxwells Road (Wharerata Forest) and for the 300 Index growth reference. The data used in the analysis starts at the vertical grey line (2005, age 15); b. Yearly basal area increments relative to the 300 Index growth reference for 39 trees at Maxwells Rd over the study period. The level corresponding to equal growth between observation and reference is depicted as a dashed black line.

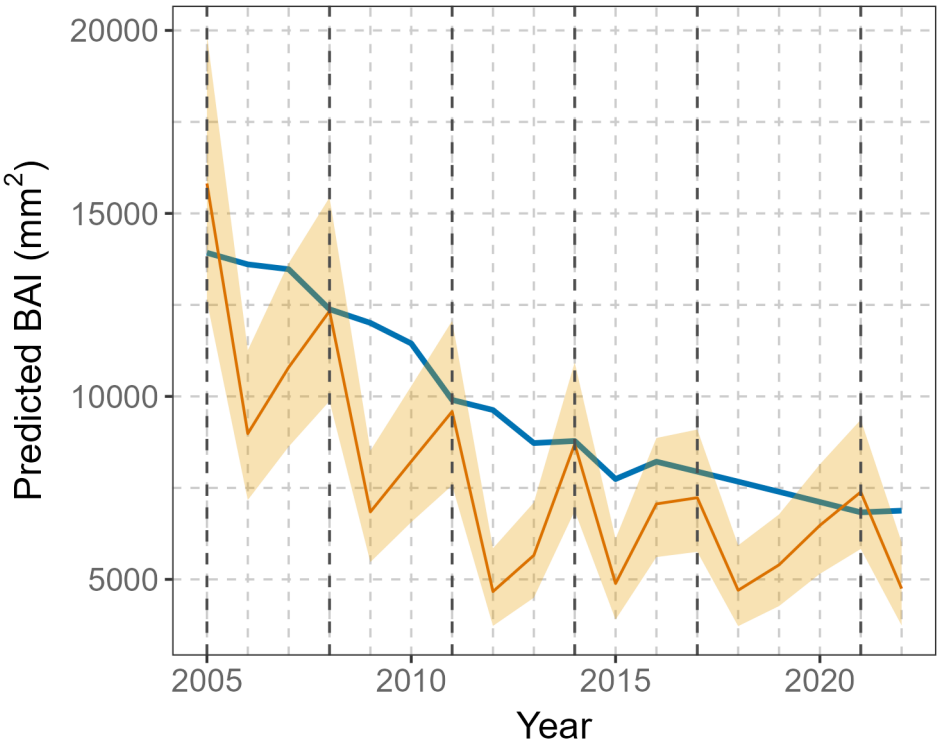

FIGURE 3: Prediction of yearly basal area increments (BAI) for average climate conditions at Maxwells Rd (Wharerata). The orange line and bands represent the posterior mean and 90% credible intervals respectively. The blue line is the 300 Index BAI growth reference. Years of RNC outbreaks are marked with vertical dashed lines.

that each additional RNC event aggravates growth loss. Outbreak 3 had the most damaging effect on growth, followed by outbreak 2 then 5. This suggests that successive disease events do not compound their effects over the long term. From Table 3, we estimated growth losses of 20.0% and 11.3% over the period of disease (2005-2022) and over the whole rotation (1990-2022), respectively.

Observed growth response to RNC severity at Kinleith

The Kinleith data only covers one main RNC event in 2016, but the collection of yearly RNC severity scores allowed the estimation of the effect of tree-level RNC severity on radial growth over 4 years. No outbreak occurred during the 2017-2021 period, although mild symptoms on some trees were observed and recorded. Figure 4 shows observed basal area increment profiles of trees from 2007 as well as the distribution of RNC severity across all trees and plots on the year of the outbreak. Trees experiencing high RNC severity generally show a slower growth after 2016 than moderately affected trees. It is also worth noting the tendency of trees having high growth rates pre-infection showing lower levels of RNC severity.

Inferred growth response to RNC severity at Kinleith

The final model predicted the log-transformed percent BAI growth of total BAI growth per tree. Predictors used were year of growth, climate, and RNC severity scores for each of 4 years prior to the year of growth. All HMC chains converged, with an appropriate posterior resolution (Table 1). Year of growth conditional on climatic conditions informs about age-related tree-specific radial growth patterns (stand age was uniform across each location) and stand-level competition dynamics. By including this variable to the model we account for any linear trend with tree/stand age and, potentially, any annual linear trend not directly related to climate conditions. In our case, year and climate might have partially confounding effects as we observed an increasing temperature trend over the study period that translated into a visible PC1 trend (data not shown). We computed growth predictions (relative to total growth) for three chosen levels of 2016 RNC severity corresponding to extreme and mid-range observed values (0%, 50%, 95%). Results are displayed in Figure 5. Growth loss estimates were inferred by computing the ratio of yearly growth proportions from each level to estimated growth proportions from the healthy level (0%), for each draw from the predictive posterior distribution. Summarised results are presented in Table 3. RNC severity had a strong negative effect on growth in the two years following the outbreak. The highest RNC severity (95%) induced a 32.8 % reduction in growth compared to healthy trees the year following disease, and a moderate severity (50%) induced a 18.9% growth reduction. The effect of RNC severity was comparable the following year and then decreased to 23.6% (95%

TABLE 3: Estimated percent growth loss for each year following an RNC outbreak at Wharerata and Kinleith, with 90% credible interval bounds. Negative values indicate growth gain relative to the healthy expectation.

Site	Outbreak No.	Year 1	Year 2	Year 3	Year 4
Wharerata	1	34 [17.3,47.3]	19.9 [-1.2,36]	0.4 [-24.7,20.3]	
	2	43 [29.1,54.4]	28.2 [10.2,42.6]	3.2 [-21.8,23.6]	
	3	51.5 [39.3,61.3]	35.2 [18.6,48.4]	1 [-24.5,21.7]	
	4	36.9 [21.1,49.6]	14 [-7.9,31.7]	9 [-14.5,27.6]	
	5	38.7 [22.7,51.5]	27 [8.4,42.2]	9 [-14.5,27.6]	-8.1 [-37,14.6]
	6	31 [12.5,45.6]			
average		39.2	24.9	4.5	-8.1

Site	Outbreak severity	Year 1	Year 2	Year 3	Year 4
Kinleith	50%	18.9 [13.4,24.4]	20.5 [14.8,26]	13.2 [6.9,19.1]	8.2 [1.7,14.5]
	95%	32.8 [25.1,40]	35.3 [27.3,42.5]	23.6 [14.6,32]	14.9 [4.8,24.2]

severity) and 13.2% (50% severity) on year 3 (Table 3). On year 4 after disease, predictions for healthy and severely affected trees still differed, with a growth loss around 15% and no overlap between 90% credible intervals (Figure 5).

Discussion

We quantified yearly growth loss following disease at two sites, showing that a single high-severity disease event can lead to 30-50% growth loss for the year after expression. Yearly growth loss is observed for 3 to 4 years after disease, showing that growth impacts remain for several years, despite crown recovery. Through a unique example of RNC infection cycle over a complete stand rotation at Wharerata, we showed that recurring disease events every three to four years can lead to a 20% reduction in total radial growth over the period encompassing the presence of the disease, but also that the effect of each successive disease event does not seem to compound towards a higher impact or slower recovery over time. Through detailed individual tree scoring over

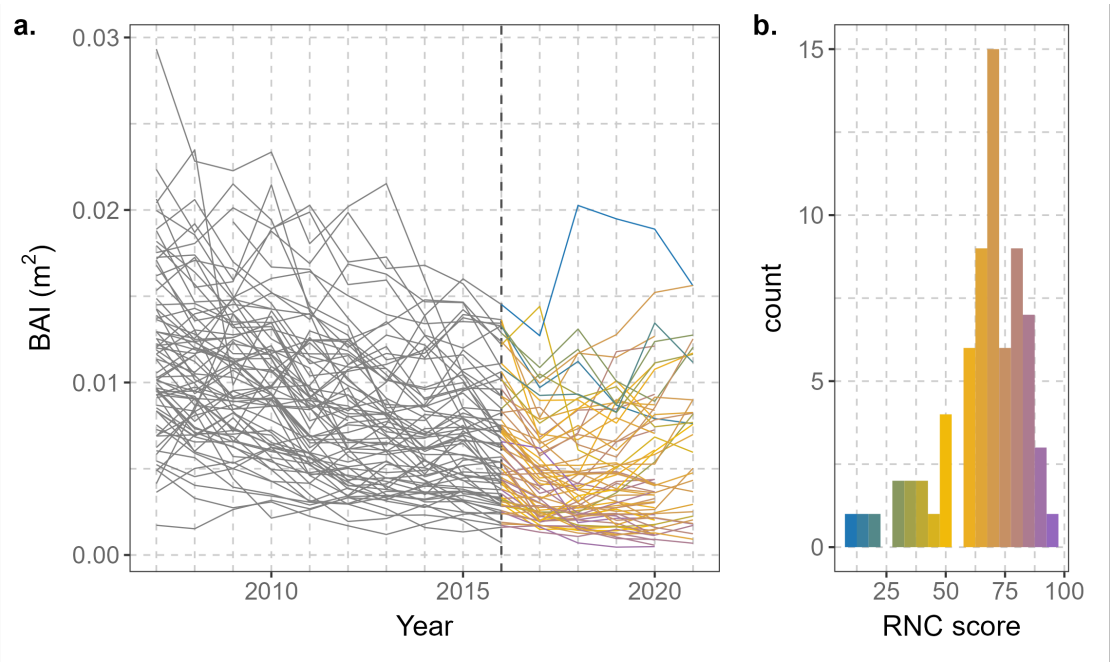

FIGURE 4: a. Yearly basal area increments from 77 trees at Kinleith. Tree series were coloured from 2016 onwards according to their 2016 RNC severity score; b. Distribution of 2016 RNC scores across 77 trees at Kinleith, showing the colour scale for a.

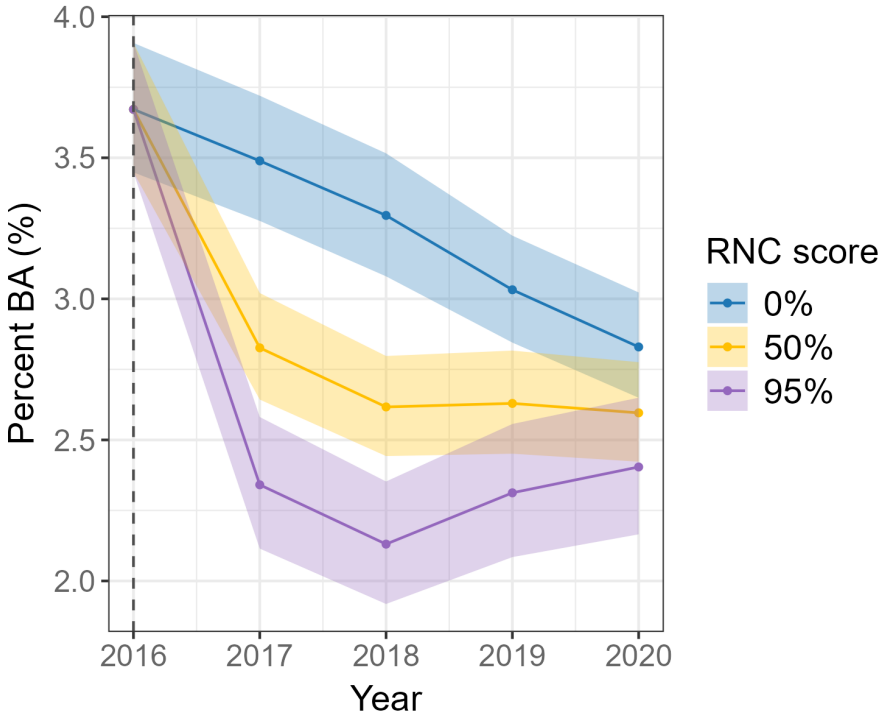

FIGURE 5: Predicted proportion of tree-level total stem basal area grown at Kinleith for the 2016 RNC outbreak and four following years, for three levels of RNC severity. Lines and bands represent the posterior mean and 90% credible intervals respectively.

several years at Kinleith, we could also relate the severity level of RNC symptoms to radial growth at the tree level. Beets (unpublished data) describes a radial growth assessment of the Maxwells Road site at Wharerata after the 2008 and 2011 RNC outbreaks, using a lesser-affected nearby stand of different age as a healthy reference with no adjustment for climatic conditions. They estimated growth loss at 38% and 10% 1 year and 2 years after outbreak respectively. These estimates are lower than those obtained in the current study for the same disease events (Table 2, Wharerata outbreaks 2 and 3). The discrepancy may be due to the use of stands that were also affected by RNC as healthy growth reference in the earlier study, but also to the limited amount of data and growth-affecting variables available for the assessment at the time. This preliminary study nonetheless formed the basis for the long-term monitoring of the stands at the Wharerata site that the current study relies on and recorded some qualitative information of importance on historical disease occurrence and severity.

Despite the different data and models used at the Wharerata and Kinleith sites, we obtained initial growth loss results of similar order, although direct comparison of estimates is impossible as we lack details about the severity of RNC outbreaks at Wharerata. Previous observations from the 2013 study mentioned above have described 2008 and 2011 outbreaks at Wharerata as "severe", suggesting growth loss estimates for these years should most likely be compared to the 95% severity estimates from Kinleith, in which case we observe a general agreement between the two case studies. However, the recovery trajectory past the first year is different between Kinleith and Wharerata outbreaks. Recovery seemed to take longer after the 2016 Kinleith outbreak compared to all six Wharerata outbreaks, with growth differences between affected trees and unaffected trees still observable 4 years after the disease event at Kinleith, whereas growth loss following outbreaks at Wharerata were barely detectable after 3 years. This could be explained by higher vigour at Wharerata than at Kinleith, making trees more resilient to disease. At equal age, the absolute stem area increments were on average higher at Wharerata than at Kinleith (Figure S1). However, care should be taken when giving biological interpretations to prediction differences, as only one disease event was observed at Kinleith, alongside a climatic trend over the study period, creating potential modelling limitations. We also observed that trees growing slower prior to disease tended to be more affected by disease at Kinleith. This dependence of disease severity on earlier growth rate might contribute to uncertainty over final growth loss estimates and to some sensitivity of estimates to modelling choices. On the other hand, our confidence in the results at the Wharerata site are strengthened by the observation of several RNC outbreaks. The lack of data past 3 years post-outbreak for 5 out of 6 RNC events is compensated by the estimation of hardly detectable growth loss three years after event and the positive growth ratio compared to reference 4 years after the 2017 outbreak. As all growth loss estimates at Wharerata are calculated based on ratios of observed growth data and simulated data

from the 300 Index growth reference, trust in the results crucially depend on trust in the reference growth curve. The accordance of average growth in sampled trees with the reference for the pre-disease period (up to 2005) provides some evidence that the reference is accurate.

Diameter growth is one of the main quantifications of radiata pine productivity. As many productivity forecasting models are based on diameter growth, findings from the current study can be incorporated in productivity forecasting tools used by forest managers in regions where the disease is present to more accurately predict productivity. Paired with spatialised tools that are currently being developed to predict RNC occurrence and severity across a whole region on a yearly basis at a high resolution (Camarretta et al. 2024; Watt et al. 2024), large-scale, year-to-year quantification of disease risks and their potential consequences will soon be available to forest managers. However, the geographic extent of available spatialised tools is currently limited to the East Coast region where the most extreme cases of disease occurrence and frequency, such as the Wharerata site studied here, have been observed. The disease levels observed at the Kinleith site may be more typical to average levels among all areas in New Zealand where RNC is present. More research needs to be conducted to precisely predict forthcoming RNC-related growth loss at the landscape level across regions. While wet and relatively cool summers seem to favour RNC outbreaks on a year-to-year basis (Watt et al. 2024), longer-term disease incidence in New Zealand is likely shifting with climate change trends, and predictions will need to be expanded to newly affected regions. Moreover, the effect of yearly weather patterns on symptom severity and tree-level recovery is currently little known but likely complex, as hypothesised by Wakelin et al. (2018). There is anecdotal evidence of drought interacting with disease-related stress and slowing down recovery (Beets, unpublished data), but data is currently insufficient to confidently quantify the relationship between the compounding impact of RNC and abiotic stressors. Finally, mortality and interaction with root disease were not considered in this and previous studies of RNC impact in New Zealand. Field observations suggest that single defoliation events do not lead to mortality, but it is possible that repeated defoliation episodes in stressed trees can ultimately cause it. Mortality attributed to armillaria root rot (ARR) at Kinleith was significant in areas severely affected by Dothistroma needle blight (Sweet 1989). Shaw and Toes (1977) found that growth loss in trees affected by both Dothistroma needle blight and ARR was greater than the additive effects of each disease alone. It is plausible that interactions between RNC and ARR would result in similar effects. If so, effective productivity losses would be greater than currently estimated. Long-term plot or stand-level monitoring is required and currently underway through disease exclusion trials in the same areas as the location of this study and will provide more precise insight into potential RNC-related mortality.

It is possible that RNC also affects aspects of tree development other than radial growth such as height growth, tree form, and wood properties. Artificial defoliation experiments have shown limited effects of lower crown defoliation on radiata pine grafts on subsequent carbon uptake (Gomez-Gallego et al. 2020). Beets (unpublished data) reports a small reduction in latewood density in RNC-affected trees but more in-depth studies need to be conducted to quantify such effects. In addition to the effect of RNC on radial growth loss, gaining knowledge on the effect of RNC on height growth would allow volume loss estimates to be made. However, studies on Cyclaneusma needle cast (Bulman & Gadgil 2001) and Dothistroma needle blight (Van der Pas 1981) showed height growth was not significantly affected by either disease. Knowing the effect of RNC on wood density and thus carbon storage loss and wood quality changes is likely of higher importance. This is especially true if the forestry industry is trying to shift its focus towards higher-quality wood products while also being used as a climate change remediation solution. In parallel to impact studies, research on mitigation tools such as relatively environmentally friendly treatment options is being conducted (Fraser et al. 2022). RNC mitigation in regions where RNC is prevalent can also be achieved through the breeding and deployment of more RNC-resistant genotypes of radiata pine, as RNC resistance is a moderately heritable trait in the New Zealand radiata pine breeding population (Dungey et al. 2014; Graham et al. 2018; Ismael et al. 2020). All these advances in impact assessment, monitoring, forecasting and mitigation will allow cost-benefit assessments of disease management interventions as well as precise and confident optimisation of silvicultural activities in regions where RNC is present.

Conclusions

By integrating extensive tree core collection and processing, long-term monitoring of disease expression, and publicly available environmental surfaces of climate profiles and site productivity in a carefully developed Bayesian statistical modelling framework, the present study reliably answers questions relating to several aspects of RNC effect on tree growth. Our findings highlight the threat of red needle cast to the forestry industry and are a first step towards cost-benefit analyses of disease management and mitigation.

Authors' contributions

LB established the Kinleith trial, LB, DL, YD, SF designed the study. DL was responsible for field collection, DL conducted wood-core processing, ring-width extraction, and preliminary analyses. JSE conducted the statistical modelling. JSE wrote the manuscript with contributions from all co-authors.

Competing interests

The authors declare that they have no competing interests.

Acknowledgements

This work formed part of the Needle Disease Strategy Project and Resilient Forests Programme, both funded by the Forest Growers Levy Trust and Scion's Strategic Science Investment Funding (from the Ministry of Business, Innovation & Employment). We thank forest owners and managers for providing access for the study and information on management regimes: Mike Baker and Nina Paton (Manulife Investment Management Forest Management), Kate Richards (née Muir) and Edward Pirini (Juken New Zealand). We thank Peter Beets for his early disease monitoring work at the Wharerata site. We also thank Gordon Tieman and Peter Scott for assisting with Kinleith disease assessments, Kane Fleet for helping with tree coring, and Damien Sellier, Michael Bartlett, and Loretta Garrett for advice.

Supplemental information

- Figure S1: Mean diameter increment with standard errors by year since establishment at Kinleith and Wharerata.
- Details on climate variables used in Kinleith and Wharerata models.

References

Bulman, L. (1993). Cyclaneusma needle-cast and Dothistroma needle blight in NZ pine plantations. *New Zealand Forestry, 38*(2), 21-24. https://nzif.org.nz/nzif-journal/publications/article/20910

Bulman, L.S., & Gadgil, P.D. (2001). *Cyclaneusma needle-cast in New Zealand*. Rotorua, New Zealand: Forest Research Institute.

Bulman, L.S., Dick, M.A., Ganley, R.J., McDougal, R.L., Schwelm, A., & Bradshaw, R.E. (2013). Dothistroma needle blight *Infectious Forest Diseases* (pp. 436-457): Wallingford UK: CABI. https://doi.org/10.1079/9781780640402.0436

Camarretta, N., Pearse, G.D., Steer, B.S., McLay, E., Fraser, S., & Watt, M.S. (2024). Automatic detection of *Phytophthora pluvialis* outbreaks in radiata pine plantations using multi-scene, multi-temporal satellite imagery. *Remote Sensing, 16*(2): 338. https://doi.org/10.3390/rs16020338

Dick, M.A., Williams, N.M., Bader, M.K.-F., Gardner, J.F., & Bulman, L.S. (2014). Pathogenicity of *Phytophthora pluvialis* to *Pinus radiata* and its relation with red needle cast disease in New Zealand. *New Zealand Journal of Forestry Science, 44*: 6. https://doi.org/10.1186/s40490-014-0006-7

Dungey, H.S., Williams, N.M., Low, C.B., & Stovold, G.T. (2014). First evidence of genetic-based tolerance to red needle cast caused by *Phytophthora pluvialis* in radiata pine. *New Zealand Journal of Forestry Science, 44*: 31. https://doi.org/10.1186/s40490-014-0028-1

Fraser, S., Gomez-Gallego, M., Gardner, J., Bulman, L.S., Denman, S., & Williams, N.M. (2020). Impact of weather variables and season on sporulation of *Phytophthora pluvialis* and *Phytophthora kernoviae*. *Forest Pathology, 50*(2): e12588. https://doi.org/10.1111/efp.12588

Fraser, S., Baker, M., Pearse, G., Todoroki, C.L., Estarija, H.J., Hood, I.A., Bulman, L.S., Somchit, C., & Rolando, C.A. (2022). Efficacy and optimal timing of low-volume aerial applications of copper fungicides for the control of red needle cast of pine. *New Zealand Journal of Forestry Science, 52*: 18. https://doi.org/10.33494/nzjfs522022x211x

Fraser, S., McLay, E., Todoroki, C., Camarretta, N., & Hood, I. (2025). Long term monitoring of red needle cast. What drives episodic outbreaks on radiata pine in New Zealand? *New Zealand Journal of Forestry Science, 55*: 12. https://doi.org/10.33494/nzjfs552025x457x

Gomez-Gallego, M., Williams, N., Leuzinger, S., Scott, P.M., & Bader, M.K.-F. (2020). No carbon limitation after lower crown loss in *Pinus radiata*. *Annals of Botany, 125*(6), 955-967. https://doi.org/10.1093/aob/mcaa013

Graham, N.J., Suontama, M., Pleasants, T., Li, Y., Bader, M.K.F., Klápště, J., Dungey, H.S., & Williams, N.M. (2018). Assessing the genetic variation of tolerance to red needle cast in a *Pinus radiata* breeding population. *Tree Genetics & Genomes, 14*(4): 55. https://doi.org/10.1007/s11295-018-1266-9

Hewitt, A.E. (2010). *New Zealand soil classification.* Lincoln, New Zealand: Manaaki Whenua Press.

Ismael, A., Suontama, M., Klapste, J., Kennedy, S., Graham, N., Telfer, E., & Dungey, H. (2020). Indication of quantitative multiple disease resistance to foliar pathogens in *Pinus radiata* D.Don in New Zealand. *Frontiers in Plant Science, 11*: 1044. https://doi.org/10.3389/fpls.2020.01044

Kimberley, M., West, G., Dean, M., & Knowles, L. (2005). The 300 index A volume productivity index for radiata pine. *New Zealand Journal of Forestry, 50*(2): 13-18. https://nzif.org.nz/nzif-journal/publications/article/22281

Kimberley, M., Hood, I., & Knowles, R. (2011). Impact of Swiss needle-cast on growth of Douglas-fir. *Phytopathology, 101*(5), 583-593. https://doi.org/10.1094/PHYTO-05-10-0129

Landcare Research NZ. (2019). *S-map - New Zealand's national digital soil map.* https://smap.landcareresearch.co.nz Retrieved on 13 November 2024.

Van der Pas, J. (1981). Reduced early growth rates of *Pinus radiata* caused by *Dothistroma pini*. *New Zealand Journal of Forestry Science, 11,* 210-220, https://www.scionresearch.com/__data/assets/pdf_file/0017/59300/NZJFS1131981VANDERPAS210-220.pdf

Shaw III, C.G., & Toes, E.H. (1977). Impact of Dothistroma needle blight and Armillaria root rot on diameter growth of *Pinus radiata*. *Phytopathology, 67*, 1319-1323. https://www.apsnet.org/publications/phytopathology/backissues/Documents/1977Articles/Phyto67n11_1319.PDF

Stan Development Team (2023). Stan Reference Manual, version 2.26.1. https://mc-stan.org

Sweet, G. (1989). Keynote Address: Maintaining health in plantation forests. *New Zealand Journal of Forestry Science, 19*(2/3), 143-154. https://www.scionresearch.com/__data/assets/pdf_file/0012/59997/NZJFS192-and-31989SWEET143_154.pdf

Wakelin, S.A., Gomez-Gallego, M., Jones, E., Smaill, S., Lear, G., & Lambie, S. (2018). Climate change induced drought impacts on plant diseases in New Zealand. *Australasian Plant Pathology, 47*, 101-114. https://doi.org/10.1007/s13313-018-0541-4

Wang, T., Wang, G., Innes, J.L., Seely, B., & Chen, B. (2017). ClimateAP: an application for dynamic local downscaling of historical and future climate data in Asia Pacific. *Frontiers of Agricultural Science and Engineering, 4*(4), 448-458. https://doi.org/10.15302/J-FASE-2017172

Watt, M.S., Palmer, D.J., Leonardo, E.M.C., & Bombrun, M. (2021). Use of advanced modelling methods to estimate radiata pine productivity indices. *Forest Ecology and Management, 479*: 118557. https://doi.org/10.1016/j.foreco.2020.118557

Watt, M.S., Holdaway, A., Watt, P., Pearse, G.D., Palmer, M.E., Steer, B.S.C., Camarretta, N., McLay, E., & Fraser, S. (2024). Early prediction of regional red needle cast outbreaks using climatic data trends and satellite-derived observations. *Remote Sensing, 16*(8): 1401. https://doi.org/10.3390/rs16081401

Supplemental Information

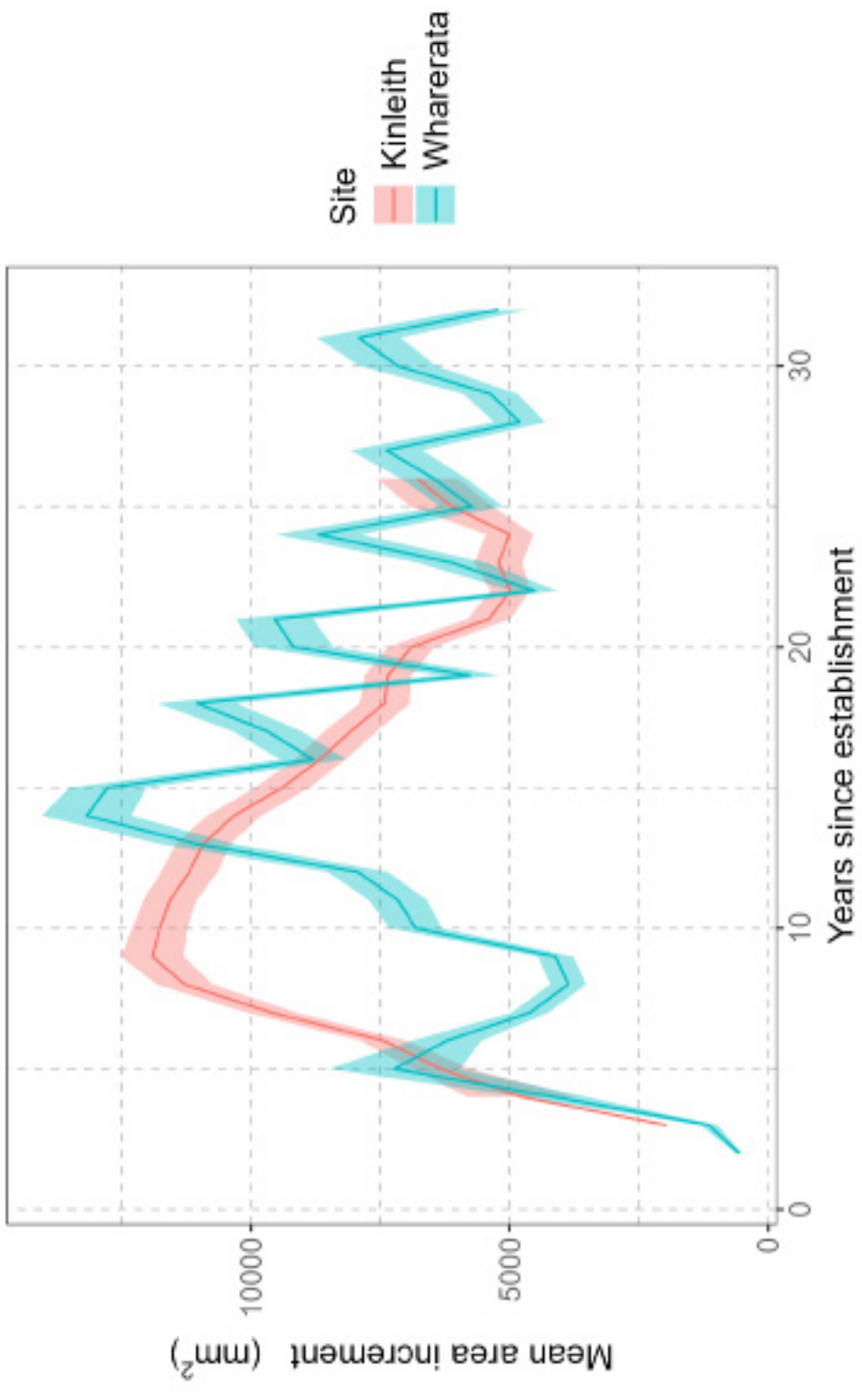

FIGURE S1: Mean diameter increment with standard errors by year since establishment at Kinleith and Wharerata.

Details on climate variables used in the Wharerata and Kinleith models

For each sampled plot location and each year of growth, annual, seasonal and monthly climate variables were extracted using the ClimateAP standalone software (Wang et al. 2017). Minima, maxima and averages for monthly and seasonal variables were used. These variables included temperature-related variables, precipitation variables, degree days below and above a set of threshold temperature, number of frost-free days, and moisture-related variables, totalling 225 variables. A Principal Component Analysis (PCA) was conducted on variables after scaling and centring, to reduce dimensionality and collinearity of the dataset.

The final number of principal components (PCs) to include in the model was decided as part of the model selection process at each site. The Kinleith models retained the 3 first PCs and the Wharerata model retained the two first PCs.

The variance explained and by each principal component for each PC (barplot) and the cumulative variance explained (dots and lines) for each model is shown in Figure S2. The shading corresponds to the PCs present in the final model.

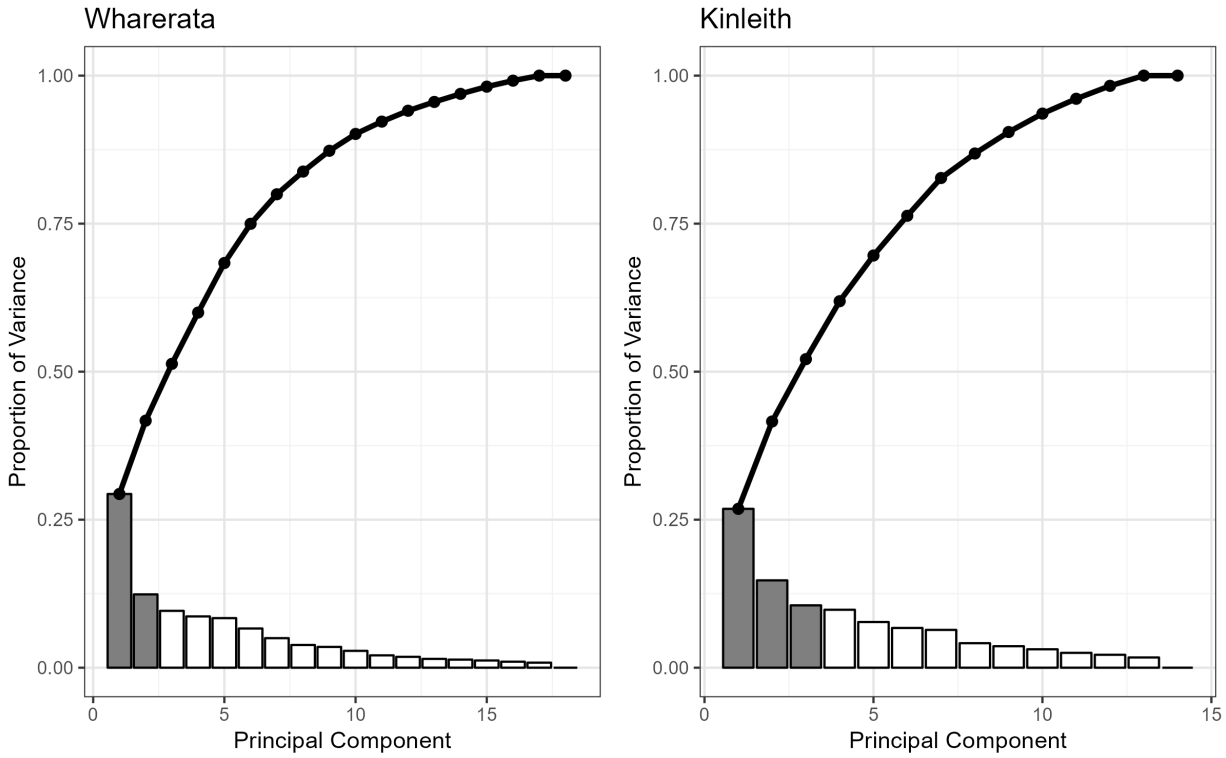

FIGURE S2: Proportion of variance explained by each climate principal component (bars) and cumulative variance explained (dots and lines) at Wharerata and Kinleith. The shaded bars correspond to principal components included in the final statistical model at each site.

Reference

Wang, T., Wang, G., Innes, J.L., Seely, B., & Chen, B. (2017). ClimateAP: an application for dynamic local downscaling of historical and future climate data in Asia Pacific. *Frontiers of Agricultural Science and Engineering, 4*(4), 448-458. https://doi.org/10.15302/J-FASE-2017172